

Apoptotic Effect of Quercetin on HT-29 Colon Cancer Cells via the AMPK Signaling Pathway

HYEONG-JIN KIM,[†] SANG-KI KIM,[†] BYEONG-SOO KIM,[†] SEUNG-HO LEE,[†]
 YOUNG-SEOK PARK,[†] BYUNG-KWON PARK,[†] SO-JUNG KIM,[†] JIN KIM,[†]
 CHANGSUN CHOI,[§] JONG-SUK KIM,[#] SUNG-DAE CHO,[‡] JI-WON JUNG,[⊗]
 KYONG-HWAN ROH,[△] KYUNG-SUN KANG,[△] AND JI-YOUN JUNG^{*†}

[†]Department of Companion and Laboratory Animal Science, Kongju National University, 340-702 Yesan, Republic of Korea, [§]Department of Food and Nutrition, College of Human Ecology, Chung-Ang University, 456-756 Ansong, Republic of Korea, [#]Department of Biochemistry, Institute of Medical Science, Chonbuk National University Medical School, 561-180 Jeonju, Republic of Korea, [‡]Department of Oral Pathology, School of Dentistry, Chonbuk National University, 561-756 Jeonju, Republic of Korea, [⊗]Division of Intractable Diseases, Center for Biomedical Sciences, National Institute of Health, 122-701 Seoul, Republic of Korea, and [△]Department of Veterinary Public Health, College of Veterinary Medicine, Seoul National University, 151-742 Seoul, Republic of Korea

Activation of AMP-activated protein kinase (AMPK), a physiological cellular energy sensor, strongly suppresses cell proliferation in both nonmalignant and tumor cells. This study demonstrates the mechanism of quercetin-induced apoptosis in HT-29 colon cancer cells. Treatment of cells with quercetin significantly decreased cell viability in a dose-dependent manner. Notably, quercetin increased cell cycle arrest in the G1 phase and up-regulated apoptosis-related proteins, such as AMPK, p53, and p21, within 48 h. Furthermore, *in vivo* experiments showed that quercetin treatment resulted in a significant reduction in tumor volume over 6 weeks, and apoptosis-related protein induction by quercetin was significantly higher in the 100 mg/kg treated group compared to the control group. All of these results indicate that quercetin induces apoptosis via AMPK activation and p53-dependent apoptotic cell death in HT-29 colon cancer cells and that it may be a potential chemopreventive or therapeutic agent against HT-29 colon cancer.

KEYWORDS: Quercetin; HT-29; AMPK; p53; p21; apoptosis; cancer; chemoprevention

INTRODUCTION

Colorectal cancer is the third most common cancer and the fourth most frequent cause of cancer deaths worldwide (1). Epidemiological studies have shown significant differences in the incidence of colon cancer among ethnic groups. The much higher incidence of colon cancer in the United States and Europe compared to Asian countries such as Japan and China is believed to be partially due to diet (2).

Recent studies in both humans and animals have shown that regular consumption of fruits, vegetables, spices, and tea provides essential nutrients and that many diet-derived phenolics, particularly flavonoids, exert potential anticarcinogenic activities and are associated with a reduced risk of cancer (3).

Quercetin (Figure 1A; 3,3',4',5,7-pentahydroxyflavone) is a major dietary flavonoid found in a wide range of fruits, vegetables, and beverages, such as tea and wine. It is often eaten daily in Western countries and is extensively metabolized in the small intestine and liver (4). Quercetin is one of the most potent antioxidants, as demonstrated in *in vitro* (5) and *in vivo* studies (6). The anti-inflammatory,

antiproliferative, and apoptotic effects of quercetin have been analyzed in cell culture models (7).

At the molecular level, quercetin acts as an anticancer agent by down-regulating the expression of oncogenes (H-ras, c-myc, and K-ras) and anti-oncogenes (p21-ras; 8,9) or up-regulating the control proteins of the cell cycle, such as p21WAF1 and p27KIP1 (10). In addition, quercetin inhibits tyrosine and serine–threonine kinases, the activities of which are linked to survival pathways such as MAPK and AKT/PKB (11).

AMP-activated protein kinase (AMPK) is a member of a family of serine–threonine protein kinases that are found in all eukaryotes (12). The unique ability of AMPK to directly sense the energy status of the cell makes it an attractive target molecule for ensuring that cell division proceeds when cells have sufficient metabolic resources to support cell proliferation (13). AMPK is also an antigrowth molecule because of its relationship to two tumor suppressor genes: LKB1 and TSC2 (tuberous sclerosis complex 2). LKB1 is the upstream activating kinase for the stress-responsive AMP-activated kinase and links regulators of cellular metabolism and cell proliferation in cancer (14). LKB1 activates AMPK and thus serves as the principal AMPKK (15–17). LKB1 also protects cells from apoptosis in response to agents that elevate

*Author to whom correspondence should be addressed (phone 82-41-330-1520; fax 82-41-330-1529; e-mail wangza@kongju.ac.kr).

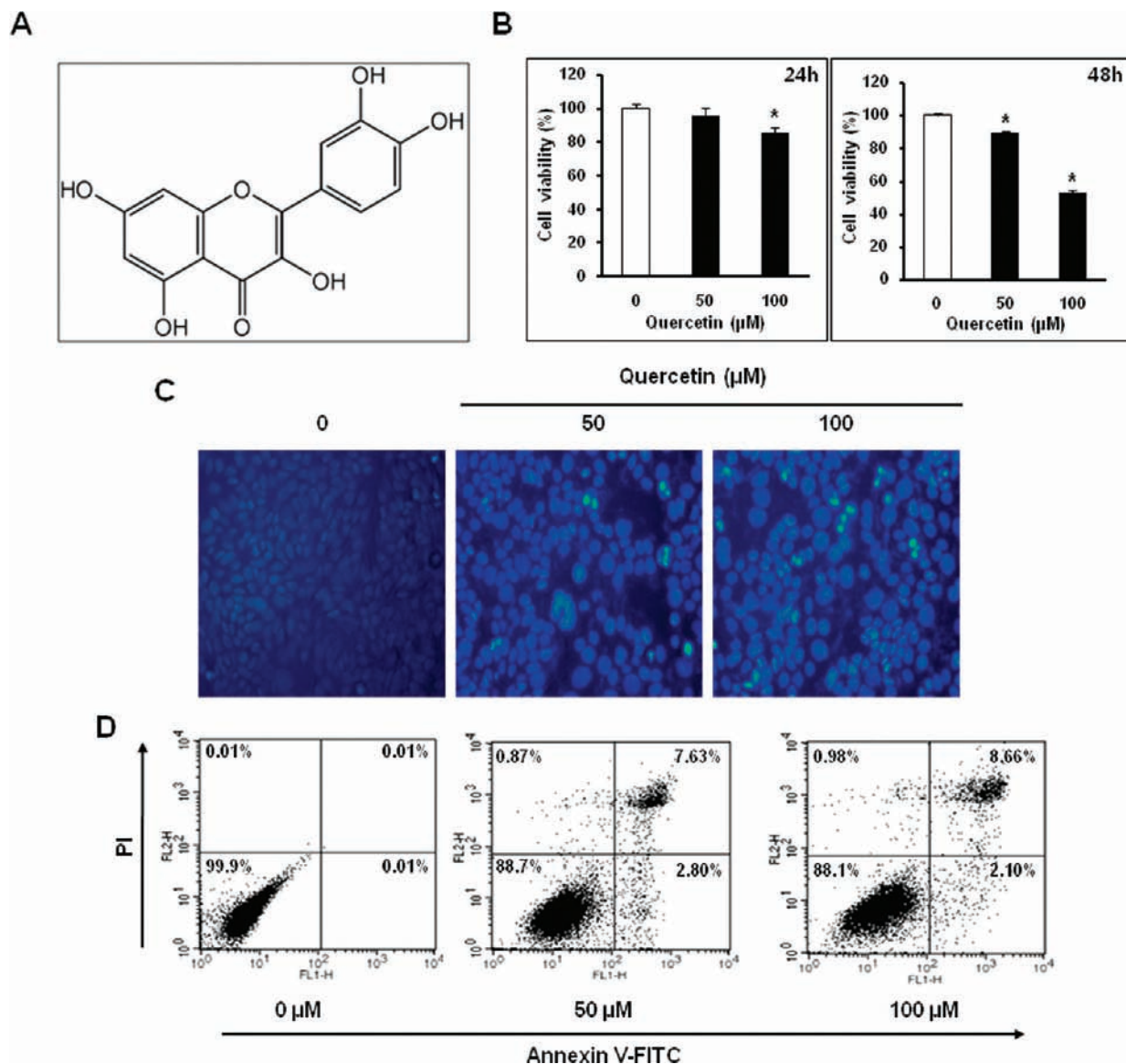


Figure 1. Effect of quercetin on viability and annexin positive apoptotic cells. Panel **A** shows the structure of naturally occurring quercetin. (**B**) HT-29 cells were treated with quercetin (0, 50, or 100 μM) for 24 or 48 h, and cell viability was determined by MTT assay as described under Materials and Methods. Each bar represents the mean \pm SE of three separate experiments, and data are expressed as percent relative to the control. (**C**) HT-29 cells were treated with 0, 50, or 100 μM quercetin for 48 h and stained with DAPI. Chromatin condensation, representing apoptotic cell death, was examined using a fluorescence microscope ($\times 400$). (**D**) Cells were treated with quercetin (0, 50, or 100 μM) for 24 h. Cells positive for either annexin V or both annexin V and PI were considered to be early apoptotic and late apoptotic cells, respectively. Labeled cells were analyzed by FACS analysis. The figure shows a representative staining profile for 10000 cells per experiment.

intracellular AMP. Embryonic fibroblasts of LKB1-deficient mice are defective in AMPK activation and undergo apoptosis under conditions that elevate AMP. Ca^{2+} /calmodulin-dependent protein kinase also regulates AMPK in cell lines that lack LKB1 expression (18).

AMPK activity requires phosphorylation of the α subunit on Thr-172 in its activation loop by one or more upstream kinases (AMPKK)(18–20). AMPK phosphorylation down-regulates ATP-consuming processes, such as the synthesis of fatty acids, cholesterol, and proteins, while up-regulating ATP-producing catabolic pathways, such as fatty acid oxidation and glucose uptake. Furthermore, AMPK activation regulates apoptosis in multiple types of cancer cells by signaling pathways, such as COX-2, Akt, and mTOR, which include the up-regulation of p53 and p21 proteins, activation of caspases, inhibition of molecules related to growth, and proliferation of cancer cells (21–23).

Many protein targets of active caspases are biologically important indicators of morphological and biochemical changes associated with apoptosis (24). Poly-ADP-ribose polymerase (PARP), one of the essential substrates cleaved by both caspase-3 and caspase-7, is an abundant DNA-binding enzyme that detects and signals DNA strand breaks (25). Release of cytochrome *c* from the internal part of the mitochondrial membrane into the cytosol results in the activation of caspases-9, -3, -6, and -7. Caspase-3 in particular is the main executor of apoptosis. Immunohistochemical analysis of the active form of caspase-3 was used to determine apoptosis in paraffin sections from various tissues (26–29).

The main goal of the present study was to determine the mechanism of quercetin-induced apoptosis in HT-29 colon cancer cells. The MTT assay was used to measure the survival rate of HT-29 cells in vitro. To evaluate whether this quercetin-induced inhibition of cell proliferation was due to cell cycle arrest and/or

apoptotic death, we assayed the cells by annexin V staining or by DNA fragment staining with propidium iodide (PI). Moreover, we used the Western blot assay to determine the relevance of each marker in apoptosis. *In vivo* studies evaluated quercetin-induced apoptosis via p53-dependent apoptotic cell death. It is not known what effects might occur if quercetin were given on the day of tumor implantation. Accordingly, tumor size was measured every 2 days after implantation of a tumor fragment into nude mice for up to 6 weeks and examined by immunohistochemical (p21, p53) and TUNEL assays to detect quercetin-induced apoptosis.

MATERIALS AND METHODS

Cells, Materials, and Chemicals. HT-29 cells representing a human colorectal adenocarcinoma cell line were obtained from the Korean Cell Line Bank. Quercetin, MTT [3-(4,5-dimethylthiazol-2-yl)-2,5-diphenyltetrazolium bromide], and PI were purchased from Sigma-Aldrich (St. Louis, MO). RPMI-1640 medium, penicillin–streptomycin, trypsin–EDTA, and fetal bovine serum (FBS) were obtained from HyClone Laboratories (Logan, UT). Polyclonal anti-PARP, anti-cleaved-PARP, anti- β -actin, anti-caspase-3, anti-cleaved-caspase-3, anti-AMPK α (Thr172), anti-phospho-AMPK α (Thr172), anti-Bax, anti-Bcl-2, and anti-p21 were purchased from Cell Signaling Technology (Danvers, MA). Anti-p53 antibody was purchased from Abcam (Cambridge, U.K.). Dimethyl sulfoxide (DMSO) was purchased from Merck (Darmstadt, Germany). Cell lysis buffer and DAPI were obtained from Invitrogen (Carlsbad, CA). A fluorescein isothiocyanate (FITC)-conjugated annexin V apoptosis detection kit was purchased from BD Bioscience (San Diego, CA).

Preparation of Quercetin. Quercetin was dissolved in DMSO prior to treatment (0, 50, or 100 μ M). The concentration of DMSO in control experiments or in experimental samples was always $1/1000$ (v/v) of the final medium volume.

Cell Culture. HT-29 cells were maintained in RPMI-1640 supplemented with 10% FBS and 1% penicillin–streptomycin (HyClone Laboratories) at 37 °C in a humidified 5% CO₂ atmosphere. For quercetin treatment, HT-29 cells were seeded at a density of approximately 3×10^4 cells/cm² in a 175 cm² flask (Nunc, Fisher Scientific, Loughborough, U.K.) and allowed to adhere overnight. The final concentration of quercetin in growth medium was 0, 50, or 100 μ M, and cells were incubated for 48 h.

MTT Cell Viability Assay. Cell survival rate was measured by the MTT assay. Cells were seeded onto 12-well microplates at 5×10^4 cells/well (24 h) or 4×10^4 cells/well (48 h) and were incubated with quercetin at concentrations of 0, 50, or 100 μ M for the indicated times. The medium was removed, and the cells were then incubated for 4 h with 1000 μ L of MTT solution (2 mg/mL MTT in PBS). Optical densities of the solutions were determined by spectrophotometer (Ultraspex 2100 pro; Amersham Biosciences, Uppsala, Sweden) at 540 nm. Cell viability was expressed as the optical density ratio of the treatment to the control.

Western Blot Assay. To harvest cells, we washed the culture flasks once with PBS and treated them with trypsin–EDTA for 2 min. Cells were gently pipetted off the flask with PBS and transferred to 15 mL conical centrifuge tubes. After centrifugation for 7 min at 1700 rpm, cell pellets were washed twice with PBS, lysed with cell lysis buffer (Invitrogen), and centrifuged at 15000 rpm for 5 min at 4 °C. Protein concentrations were measured using the Bradford protein assay (Bio-Rad, Hercules, CA) according to the manufacturer's instructions. Equal amounts of protein (10 μ g) were separated by 12% SDS-PAGE and electrophoretically transferred onto polyvinylidene difluoride membranes (Amersham Biosciences). The transferred membranes were blocked with Tris-buffered saline containing 5% nonfat dry milk and 0.1% Tween 20 at 4 °C for 2 h. After blocking, the membranes were incubated with anti-cleaved PARP, anti-PARP, anti- β -actin, anti-caspase-3, anti-cleaved-caspase-3, anti-AMPK α (Thr172), anti-phospho-AMPK α (Thr172), anti-Bax, anti-Bcl-2, anti-p21 (Cell Signaling Technology), and anti-p53 (Abcam) antibodies overnight at 4 °C with gentle shaking. After incubation with primary antibodies, the membranes were incubated with horseradish peroxidase-conjugated goat anti-mouse or anti-rabbit IgG secondary antibodies (Cell Signaling Technology) for 2 h at room temperature with gentle shaking. After washing, bands were visualized by ECL detection reagents (Pierce, Rockford, IL) according to the manufacturer's instructions. Blots were reprobed with β -actin antibody used as a loading control.

Nuclear Morphology. To assess apoptosis, we stained the nuclei of HT-29 cells with DAPI. Cells were seeded onto 12-well microplates at 4×10^4 cells/well and were incubated with quercetin at a concentration of 0, 50, or 100 μ M for 48 h. After treatment, cells were fixed in PBS containing 4% paraformaldehyde for 30 min in an incubator. After fixation, cells were washed twice with PBS, and cell nuclei were stained with DAPI in PBS. Fluorescence was observed using a fluorescence microscope ($\times 400$).

Annexin V Staining for Analysis of Apoptosis. After stimulation of HT-29 cells with quercetin, cell apoptosis was measured with an annexin V staining kit (Becton Dickinson). HT-29 cells (including floating cells) grown in a 75 cm² flask were collected following mild trypsinization. Following the manufacturer's instructions, we washed trypsinized cells once with PBS, resuspended them in 100 μ L of annexin binding buffer, and mixed them with 5 μ L of FITC-conjugated annexin V and phycoerythrin-conjugated PI. Resuspended cells were incubated at room temperature in the dark for 15 min. Labeled cells were analyzed using FACSCalibur (Becton Dickinson).

Flow Cytometric Analysis of the Cell Cycle. The cell cycle phase was assayed by measuring DNA fragment staining with PI. HT-29 cells (including floating cells) grown in a 75 cm² flask were collected following mild trypsinization. Collected cells were centrifuged for 7 min at 1700 rpm. The cell pellets were washed twice with PBS and fixed with 70% ethanol for 30 min. After fixation, DNA fragments were stained in PBS containing 50 μ g/mL PI and 100 μ g/mL RNase (Sigma-Aldrich) for 30 min at room temperature. After sorting out viable cells, we measured fluorescence intensity using FACSCalibur (Becton Dickinson).

Animals. Thirty 5-week-old male nude mice (*nu/nu*) were obtained from the animal production company of Orient-Bio (Gyeonggi-do, Korea). The mice were maintained at a temperature of 23 ± 5 °C and a relative humidity of $40 \pm 10\%$ with artificial lighting from 8:00 a.m. to 8:00 p.m. in facilities approved by the Companion and Laboratory Animal Science Department of Kong-Ju National University. The animals were kept in cages and were allowed free access to sterilized water and commercial rodent chow (Biopia, Korea). All animal experiments were performed with the approval of the Institutional Animal Care and Use Committee and following the guidelines of Kong-Ju National University.

Colon Tumor Xenografts. HT-29 cells were maintained in RPMI-1640 supplemented with 10% FBS and 1% penicillin–streptomycin at 37 °C in a humidified 5% CO₂ atmosphere. HT-29 cells were harvested from cultures by exposure to 0.25% trypsin. Trypsinization was stopped with a solution containing 10% FBS, and cells were then washed twice and resuspended in RPMI-1640 medium. A total of 5×10^5 cells in 0.2 mL of medium was injected subcutaneously into the right flank of donor nude mice. Seven days after the subcutaneous injection, HT-29 cells growing under the skin of nude mice established tumors. When the tumor reached about 1000 mm³ in size, the mice were anesthetized with diethyl ether, and the tumor mass was surgically obtained. After slicing the mass into 2×2 mm pieces using a grid, we surgically implanted a tumor fragment into the subcutaneous tissue of the right flank of each mouse.

Preparation and Administration of Quercetin. Quercetin (0, 50, or 100 μ M) was dissolved in 5% ethanol prior to treatment. Groups of five mice each were randomly assigned to receive one of the following treatments starting on the day of implantation of the tumor fragment: Control mice were administered 5% ethanol (0.2 mL/day) every day for 6 weeks. Low-dosage mice were administered 50 mg/kg quercetin every day for 6 weeks. High-dosage mice were administered 100 mg/kg quercetin every day for 6 weeks.

Measurement of Tumor Size. Mice were monitored for up to 6 weeks after implantation, and tumor size was measured in two dimensions every other day starting on day 1 for up to 6 weeks. Tumors were measured using vernier calipers (Mitutoyo, Japan), and tumor size was calculated as $(\text{length} + \text{width}) \times 0.5^3$.

Immunohistochemistry. When tumors reached about 1000 mm³ in size, animals were euthanized by overdose of inhalation anesthesia. To detect p21 and p53, we excised tumors and fixed them in 10% buffered formalin for 7 days; successively dehydrated them in 50, 70, 95, and 100% ethanol solutions for 15 min each; and then submerged them in xylene twice for 10 min. Paraffin-embedded tissue blocks were prepared with a machine embedding center (Shandon) and cut with a microtome (Shandon). Then 5 μ m thick sections were placed on glass slides and stretched on a slide heating plate at 43 °C. The glass slides were incubated in a paraffin oven at 37 °C for 1 day. The sections were deparaffinized with two changes

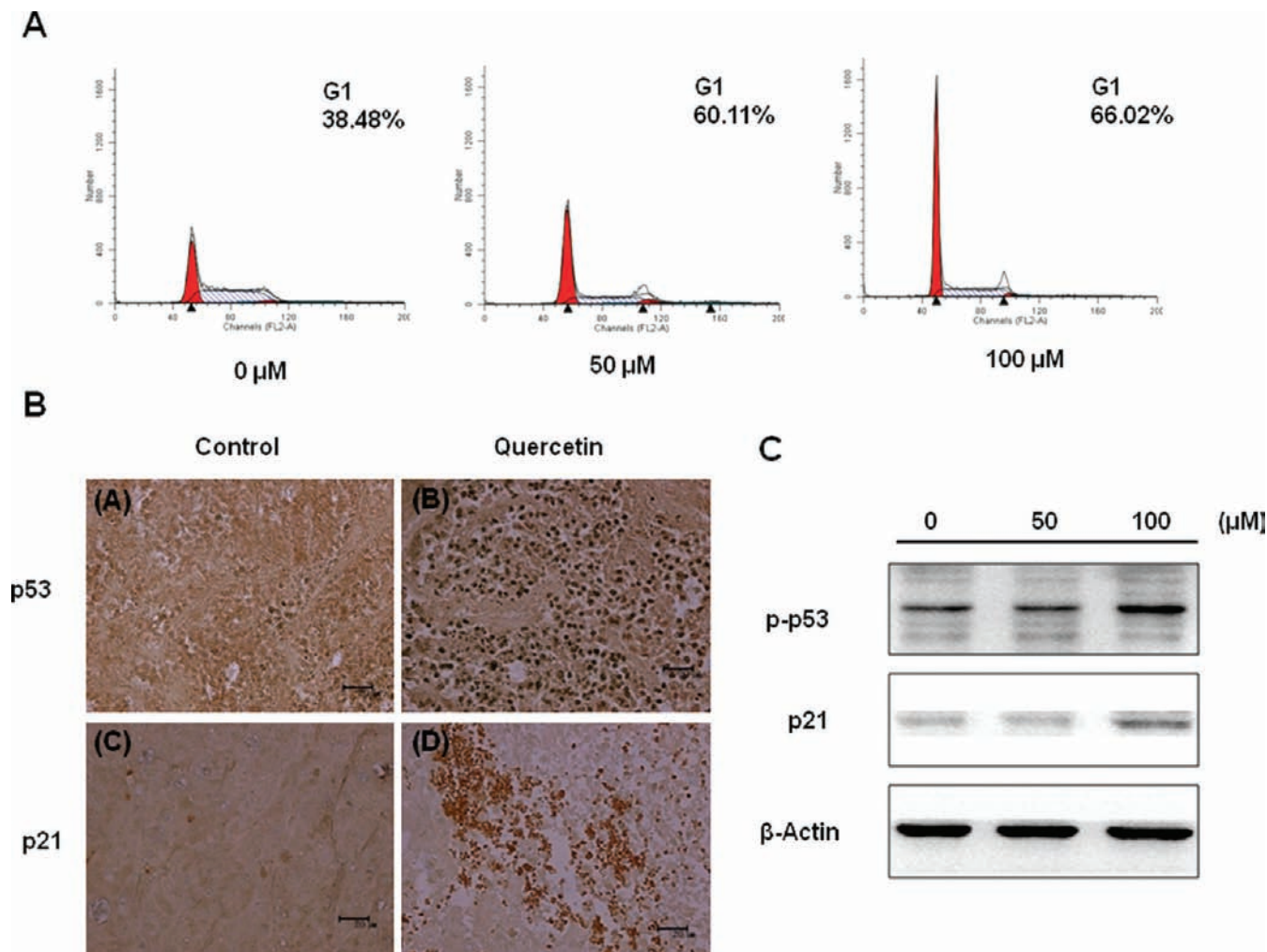


Figure 2. Effect of quercetin on cell cycle arrest and p53, p21 expression in HT-29 colon tumors. **(A)** HT-29 cells were treated with quercetin (0, 50, or 100 μM) for 24 h, and harvested cells were fixed with 70% ethanol and stained with 50 $\mu\text{g}/\text{mL}$ PI. The figure shows a representative staining profile for 10000 cells per experiment. The red spike is the cell population in G1 phase. **(B)** Nude mice were administrated quercetin (0, 100 mg/kg) for 6 weeks and assayed by immunohistochemistry using p53, p21 antibodies overnight and incubated for 1 h at room temperature with a peroxidase-conjugated goat anti-mouse antibody followed by incubation for 1 h. Subsequently, sections were stained with methyl green, treated with a mounting reagent (O. Kindler, Freiburg im Breisgau, Germany), and observed under a microscope. **(C)** Cells were treated with quercetin (0, 50, or 100 μM) for 48 h. Cell lysates were prepared as described under Materials and Methods and analyzed by 12% SDS-PAGE followed by Western blot assay. The membranes were incubated with anti-p53 and anti-p21 antibodies overnight. The blot was also probed with anti- β -actin antibody to confirm equal loading of samples.

of xylene for 10 min, rehydrated with two changes each of 100% ethanol and 95% ethanol for 1 min, and then rinsed with tap water for 10 min. The sections were incubated at 4 $^{\circ}\text{C}$ with anti-p21 (Cell Signaling Technology) and anti-p53 (Abcam) antibodies overnight and incubated for 1 h at room temperature with a peroxidase-conjugated goat anti-mouse antibody followed by incubation for 1 h. Subsequently, sections were stained with methyl green, treated with a mounting reagent (O. Kindler, Freiburg im Breisgau, Germany), and observed under a microscope.

Apoptotic Cell Detection (TUNEL). Tissue sections attached to microscope slides were deparaffinized by immersion in fresh xylene in a Coplin jar. Then the slides were washed with 100% ethanol, and the samples were rehydrated by sequential immersion in graded ethanol washes (95, 85, 70, and 50%). Apoptotic cells were detected using the Dead End Colorimetric TUNEL System (Promega, Madison, WI) according to the manufacturer's instructions. After TUNEL sections were visualized in 3'-diaminobenzidine tetrahydrochloride (DAB) solution, 50 μL of DAB substrate 20 \times buffer was added to 950 μL of deionized water. Then 50 μL of DAB 20 \times chromagen and 50 μL of hydrogen peroxide 20 \times were added. Next, 100 μL of DAB solution was added to each slide and developed until there was a light brown background, keeping it away from light for 10 min. Sections were stained with methyl green, the number of positive cells for each antibody was calculated on immunostained sections under a light microscope ($\times 200$), and the mean value was calculated for each animal.

Statistical Analysis. All data are expressed as the mean \pm SE. One-way analysis of variance was used to analyze differences among multiple comparisons. $P < 0.05$ was considered to be statistically significant.

RESULTS

Quercetin Inhibits Cell Proliferation and Induces Apoptotic Cell Death. To test the chemopreventive effects of the natural compound quercetin on the proliferation of HT-29 cells, we treated cells with various concentrations of quercetin (0, 50, or 100 μM) for 24 or 48 h and analyzed the surviving cells using the MTT assay. As shown in **Figure 1B**, quercetin induced cell death in a dose- and time-dependent manner. Treatment with 100 μM quercetin for 24 or 48 h resulted in significant decreases in cell viability compared to the control group ($P < 0.05$). The rate of cell viability was 85.7% in the 24 h stimulation group, but 52.7% of the cells survived in the 48 h stimulation group. Treatment with 50 μM quercetin slightly reduced cell viability according to culture time, with 95.6% of the cells surviving after 24 h and 89.2% of cells surviving after 48 h. These results suggest that quercetin induces cell death and inhibits cell proliferation in a dose- and time-dependent manner.

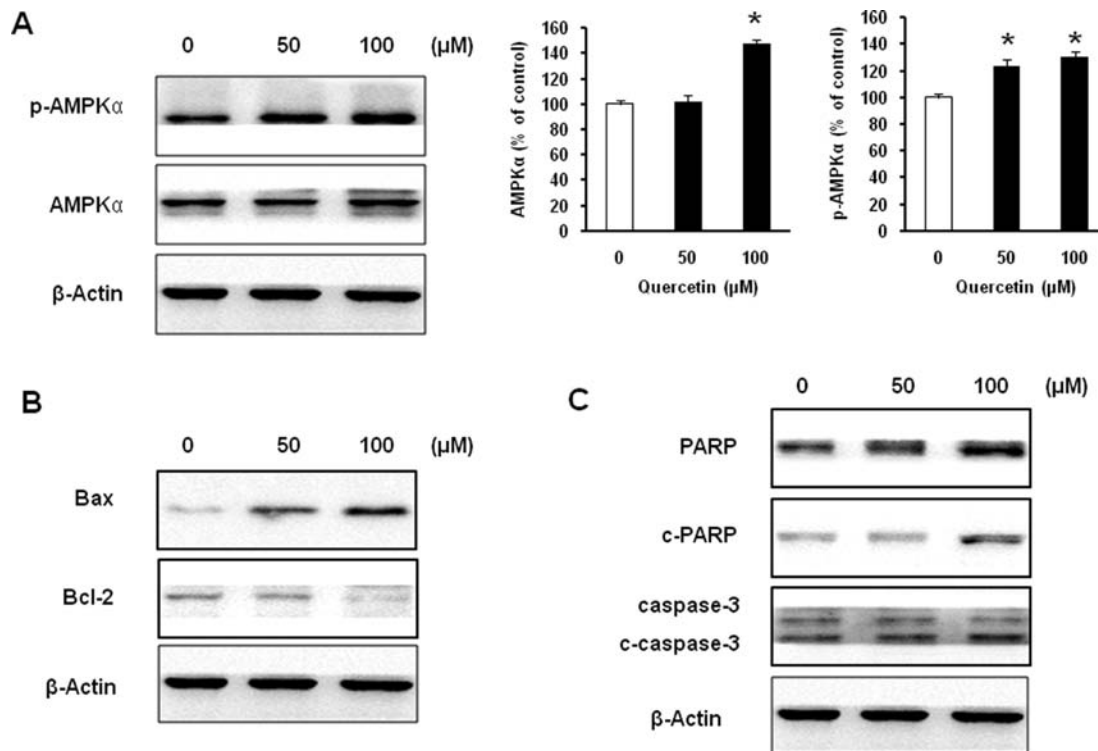


Figure 3. Effect of quercetin on the phosphorylation of AMPK. **(A)** Cells were treated with quercetin (0, 50, or 100 μM) for 48 h. Cell lysates were prepared as described under Materials and Methods and analyzed by 12% SDS-PAGE followed by Western blot assay. The membranes were incubated with anti-phospho-AMPK α (Thr172) and anti-AMPK α (Thr172); **(B)** anti-Bax and anti-Bcl-2 antibodies; **(C)** anti-PARP, anti-cleaved PARP, anti-caspase-3, and anti-cleaved-caspase-3 antibodies. The blot was also probed with anti- β -actin antibody to confirm equal loading of samples.

Quercetin Induces Chromatin Condensation in HT-29 Cells. To evaluate the effects of quercetin on chromatin condensation, we treated HT-29 cells with 50 or 100 μM quercetin for 48 h and examined them for apoptosis using DAPI staining, which distinguishes live from apoptotic cells on the basis of nuclear morphology. The presence of chromatin condensation in the quercetin-treated cells was detected on a fluorescent microscope ($\times 400$). DAPI forms fluorescent complexes with double-I banded DNA, and stained nuclei show a bright fluorescence with a DAPI filter. As shown in **Figure 1C**, cells treated with 100 μM quercetin fluoresced brightly, indicating chromatin condensation.

Quercetin Induces Apoptosis. To further understand whether quercetin-induced cell death is mediated by apoptosis or necrosis, we evaluated apoptotic cell death using annexin V/PI double staining, which specifically labels apoptotic cells. **Figure 1D** shows that quercetin treatment at concentrations of 50 and 100 μM induced apoptosis in 10.43 and 10.76% of the cells, respectively, after 24 h. However, only 0.98% of the total cell population showed necrotic cell death.

Quercetin Induces Cell Cycle Arrest at the G1 Phase. To evaluate whether this quercetin-induced inhibition of cell proliferation was due to cell cycle arrest, we maintained HT-29 cells in 50 or 100 μM quercetin for 24 h and then stained them with PI. Afterward, we analyzed the cell cycle distribution using flow cytometry. Treatment with quercetin significantly increased the G1 DNA content in HT-29 cells (**Figure 2A**). In the 50 and 100 μM quercetin treatments, the G1 population was increased, and the population in S phase was correspondingly decreased in a dose-dependent manner. The G1 population increased from 38.48 to 60.11% as a result of 50 μM treatment and from 38.48 to 66.02% as a result of 100 μM treatment. These results suggest that quercetin arrests the cell cycle in the G1 transition checkpoint in a dose-dependent manner and that this arrest is the main result of the antiproliferative effects of quercetin.

Effects of Quercetin on p21 and p53 Levels in HT-29 Colon Tumor Cells. To assess the increase in apoptosis-related proteins in quercetin-treated HT-29 colon tumors, we administered quercetin (0, 50, or 100 mg/kg) to three groups of five mice each for 6 weeks. When the control group tumors reached about 1000 mm^3 in size, the animals were sacrificed and 5 μm sections were prepared. As shown in **Figure 2B** (upper panel), the expression of p53 was significantly higher in the 100 mg/kg treated group than in the control group. Similar results were observed for p21 (**Figure 2B**).

Phosphorylation of AMPK Is Essential for Quercetin-induced Apoptosis. In cells treated with 100 μM quercetin, phosphorylation of p53 proteins was significantly increased after 48 h, and up-regulation of p21 was also observed. In contrast, no significant changes were apparent in nontreated control cells after 48 h (**Figure 2C**). To confirm whether the phosphorylation of AMPK was essential for quercetin-induced apoptosis, we treated HT-29 cells with various concentrations of quercetin (0, 50, or 100 μM) for 48 h and analyzed apoptosis-related proteins using Western blotting. As shown in **Figure 3A**, AMPK α phosphorylation at Thr-172 was significantly increased in a dose-dependent manner. This indicates that quercetin treatment results in a marked elevation of AMPK phosphorylation within 48 h. The expression of p53 downstream effectors such as Bax and Bcl-2 is key in cell cycle arrest and apoptotic death. As shown in **Figure 3B**, the total protein concentration of Bcl-2 was decreased, and Bax protein was increased in quercetin-treated cells. In addition, a marked increase in cleaved-PARP and cleaved-caspase-3 was observed in the quercetin-treated cells (**Figure 3C**). These results indicate that quercetin induces apoptosis via phosphorylation of AMPK and p53.

Effects of Quercetin on the Growth of HT-29 Colon Tumors. To assess the effects of quercetin on HT-29 colon tumor growth, we measured tumor size every 2 days after implantation into mice for

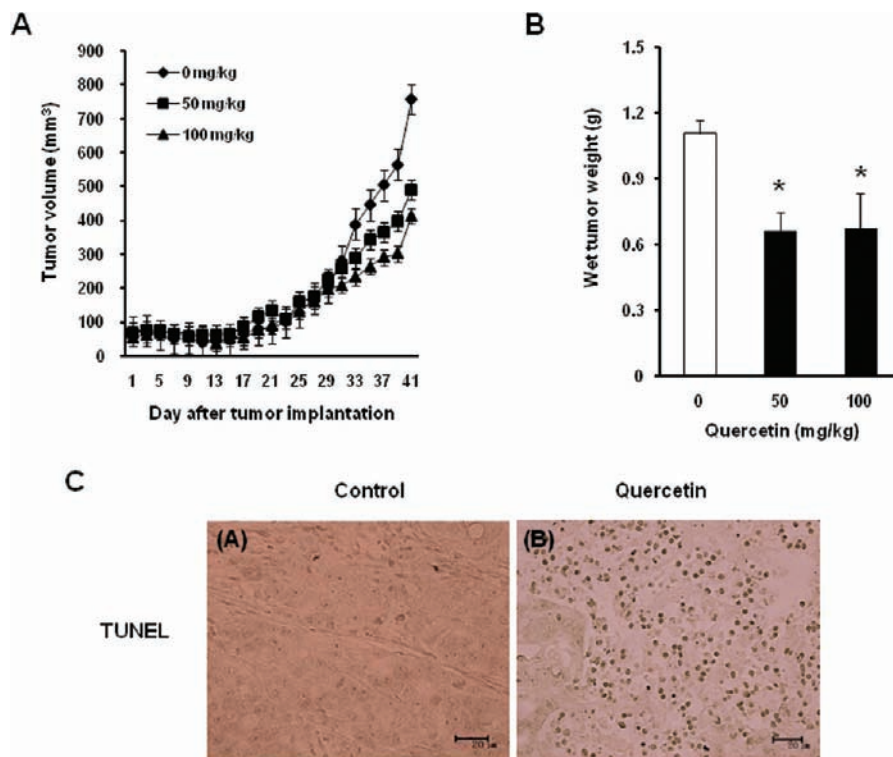


Figure 4. Effect of quercetin on HT-29 colon tumor growth and apoptosis in HT-29 colon tumors. (A) To assess the effects of quercetin on HT-29 colon tumor growth, mice were treated with quercetin (0, 50, or 100 mg/kg) for 41 days, and tumors were measured using vernier calipers. (B) Final tumor weights are graphed; each value represents the mean \pm SE for five mice. (C) Nude mice were administered quercetin (0, 50, or 100 mg/kg) for 6 weeks and TUNEL assayed as described under Materials and Methods (A, 0 mg/kg; B, 100 mg/kg). Slides were observed under a microscope and photographed ($\times 400$). Paraffin-embedded tumors were sectioned ($5 \mu\text{m}$). Scale bar = $20 \mu\text{m}$.

Table 1. Effect of Quercetin on Inhibition of HT-29 Colon Tumors

group	pre-experiment		postexperiment		inhibition rate ^a (%)
	n	size (mm ³)	n	size (mm ³)	
0 mg/kg	5	72.26	5	757.52	
50 mg/kg	5	68.41	5	491.22	35.15
100 mg/kg	5	52.54	5	413.11	45.46

^a Data are expressed as percent relative to the control.

up to 6 weeks. As described in **Figure 4A**, tumor volume was significantly decreased in the 50 and 100 mg/kg quercetin treated groups compared to the control group ($P < 0.05$). Quercetin also inhibited tumor weight in HT-29 cell xenograft (**Figure 4B**). As shown in **Table 1**, the groups given quercetin showed a significant reduction in tumor volume at day 41: 35% for the 50 mg/kg group and 45% for the 100 mg/kg group compared to the control group (0 mg/kg; both $P < 0.05$).

Effects of Quercetin on Apoptosis in HT-29 Colon Tumor Cells.

As shown in **Figure 4C**, a significant increase in TUNEL positive cells was seen in the 100 mg/kg treated group compared to the control group ($P < 0.05$). These in vivo findings support the in vitro findings that quercetin increases apoptosis in HT-29 colon tumor cells.

DISCUSSION

This study demonstrates the mechanism of quercetin-induced apoptosis via AMPK activation and p53-dependent apoptotic cell death in HT-29 cells and shows that the mechanism of cell cycle arrest is AMPK phosphorylation (see **Figure 5**). Several studies have demonstrated the relationship between cancer and diet by showing that quercetin, a major dietary flavonoid, has antiproliferative effects (3).

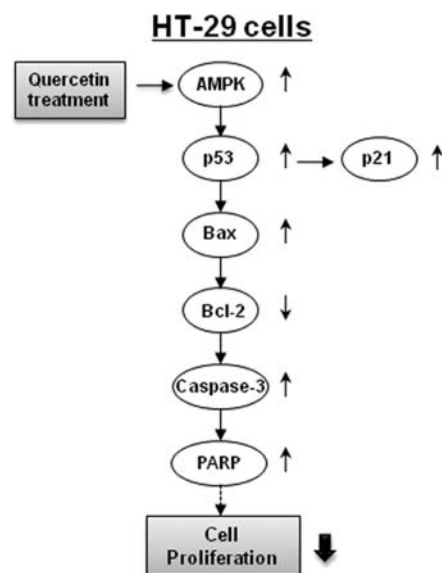


Figure 5. Possible role of quercetin in the AMPK pathway in HT-29 cells.

To test the effect of quercetin on the proliferation of HT-29 cells, we performed an MTT assay. As shown in **Figure 1B**, quercetin significantly decreased HT-29 cell viability in a dose-dependent manner. Similar effects of quercetin on leukemia (30) and prostate (31), breast (32), and lung (33) cancer cells have been reported. To further understand whether this quercetin-induced inhibition of cell viability is due to cell cycle arrest and/or apoptosis, we performed PI staining. As shown in **Figure 2A**, quercetin treatment significantly increased cell cycle arrest in the

G1 phase and up-regulated apoptosis-related proteins, such as p-p53 and p21, within 48 h (Figure 2C).

Western blot and flow cytometric analysis showed that the inhibition of p21-ras expression by quercetin was time- and concentration-dependent (8).

Flow cytometric analysis revealed that p53 strongly increased the number of cells with G1 DNA content in response to quercetin treatment via increases in p21 levels. Quercetin had no effect on the cell cycle progression in the S phase and the G₂/M phase, and the growth inhibitory effect of quercetin was the result of the arrest in the G₁ phase of the cell cycle in gastric cancer cell (34). Several studies of G1 DNA have shown that quercetin blocks the cell cycle in the G1 phase in endometrial (35) and hepatic (36) cancer cells. Up-regulation of p53 and p21 proteins leads to an inhibition of growth and proliferation in cancer cells (21–23). The increase in levels of p21, a key downstream target of p53 and one of the cyclin-dependent kinase inhibitors, mediates both G1 and G₂/M phase arrest, which is implicated in p53-dependent cell cycle arrest (37–39).

Similar results were observed in the annexin V and PI staining assays. Figure 1D shows that treatment with quercetin induced apoptosis in 10.76% of HT-29 cells after 24 h. However, only 0.98% of the total cell population showed necrotic cell death. These results indicate that the cytotoxicity caused by quercetin is mediated by apoptosis.

Apoptosis is the result of a highly complex cascade of cellular events characterized by chromatin condensation, DNA fragmentation, and cell shrinkage (40, 41). To evaluate the effect of quercetin on chromatin condensation, we performed DAPI staining. DAPI forms fluorescent complexes with double-stranded DNA, and stained nuclei brightly fluoresce under a DAPI filter. As shown in Figure 1C, cells treated with 100 μM quercetin fluoresced brightly, indicating chromatin condensation.

To confirm whether the phosphorylation of AMPK is essential for quercetin-induced apoptosis, we performed Western blot assays. AMPK activation regulates apoptosis in various types of cancer cells, and up-regulation of p53 is associated with a significant induction of AMPK phosphorylation (42). As shown in Figure 3A, phosphorylation of AMPK was induced following quercetin treatment. Phospho-p53 was also induced by treatment with quercetin. It was associated with the up-regulation of pro-apoptotic Bax (42, 43). Pro-apoptotic Bax is one of the direct targets of p53, Bax is an apoptotic protein, and Bcl-2 an anti-apoptotic protein (37). The Western blot assay revealed that quercetin increased Bax levels and reduced the total levels of Bcl-2 protein in HT-29 cells (Figure 3B).

A change in the ratio of Bax/Bcl-2 initiates caspase signaling. In other words, quercetin increased the ratio of Bax/Bcl-2, resulting in a consequent activation of caspase-3. Quercetin treatment increased cleaved-caspase-3 or cleaved-PARP in HT-29 cells (Figure 3C). Proteolytic cleavage of PARP, one of the substrates of the activated caspase-3, was induced in response to quercetin treatment; the induction of PARP is considered the point of no return in the apoptotic signaling cascade (44).

The purpose of our in vivo experiments was to examine the mechanism of quercetin-induced apoptosis via p53-dependent apoptotic cell death in nude mice. To assess the effects of quercetin in reducing HT-29 colon tumor volume, we administered quercetin (0, 50, or 100 mg/kg) to three groups of five mice each for 6 weeks. As shown in Figure 4A, the groups given quercetin showed a significant reduction in tumor volume at day 41: 35% for the 50 mg/kg group and 45% for the 100 mg/kg group compared to the control group (0 mg/kg; both $P < 0.05$). Quercetin was shown to significantly decrease tumor weights (Figure 4B). Several studies have indicated that polyphenols, including quercetin,

can inhibit cancer cell invasion (45). Resveratrol, quercetin, and catechins are absorbed and metabolized rapidly in vivo (46–50).

Inhibition of cell proliferation and induction of apoptosis in tumors are effective ways to decrease tumor growth. Phospho-p53 is a well-known transcription factor that can modulate the apoptotic process and that is involved in the anticancer activity of most anticancer agents (51). In this study, we found that apoptosis-related protein induction by quercetin was significantly higher in tissues in the 100 mg/kg treated group than in the control group (Figure 2B), and an increase in TUNEL positive cells was found in the 100 mg/kg treated tumors compared to the control tumors (Figure 4C). The control group did not show an induction of apoptosis in HT-29 colon tissues. These in vivo results support the in vitro results and suggest that quercetin induces apoptotic cell death in HT-29 colon tumor cells by p53-dependent apoptotic cell death. The effect of quercetin on AMPK is already published (52). In the present study, however, we focused on the in vivo experiment to confirm the above-mentioned report, they did not mention in vivo effects of quercetin on HT-29 colon cancer such as inhibition of tumor size or immunohistochemical findings. Our results demonstrate that oral administration of quercetin showed a significant reduction in tumor volume and TUNEL positive cells, p53 and p21, in 100 mg/kg treated group compared to the control group. These in vivo findings are novel and support the in vitro findings.

All of these results indicate that quercetin may be a potential chemopreventive or therapeutic agent against HT-29 colon cancer.

LITERATURE CITED

- (1) Weitz, J.; Koch, M.; Debus, J.; Hohler, T.; Galle, P. R.; Buchler, M. W. Colorectal cancer. *Lancet* **2005**, *365*, 153–165.
- (2) Potter, J. D.; Slattery, M. L.; Bostick, R. M.; Gapstur, S. M. Colon cancer: a review of the epidemiology. *Epidemiol. Rev.* **1993**, *15*, 499–545.
- (3) Watson, W. H.; Cai, J.; Jones, D. P. Diet and apoptosis. *Annu. Rev. Nutr.* **2000**, *20*, 485–505.
- (4) Spencer, J. P.; Chowrimootoo, G.; Choudhury, R.; Debnam, E. S.; Srai, S. K.; Rice-Evans, C. The small intestine can both absorb and glucuronidate luminal flavonoids. *FEBS. Lett.* **1999**, *458*, 224–230.
- (5) Russo, M.; Palumbo, R.; Tedesco, I.; Mazzarella, G.; Russo, P.; Iacomino, G.; Russo, G. L. Quercetin and anti-CD95(Fas/Apo1) enhance apoptosis in HPB-ALL cell line. *FEBS. Lett.* **1999**, *462*, 322–328.
- (6) Prior, R. L. Fruits and vegetables in the prevention of cellular oxidative damage. *Am. J. Clin. Nutr.* **2003**, *78*, 570–578.
- (7) Lamson, D. W.; Brignall, M. S. Antioxidants and cancer, part 3: quercetin. *Altern. Med. Rev.* **2000**, *5*, 196–208.
- (8) Ranelletti, F. O.; Maggiano, N.; Serra, F. G.; Ricci, R.; Larocca, L. M.; Lanza, P.; Scambia, G.; Fattorossi, A.; Capelli, A.; Piantelli, M. Quercetin inhibits p21-RAS expression in human colon cancer cell lines and in primary colorectal tumors. *Int. J. Cancer* **2000**, *85*, 438–445.
- (9) Avila, M. A.; Velasco, J. A.; Cansado, J.; Notario, V. Quercetin mediates the down-regulation of mutant p53 in the human breast cancer cell line MDA-MB468. *Cancer Res.* **1994**, *54*, 2424–2428.
- (10) Casagrande, F.; Darbon, J. M. Effects of structurally related flavonoids on cell cycle progression of human melanoma cells: regulation of cyclin-dependent kinases CDK2 and CDK1. *Biochem. Pharmacol.* **2001**, *61*, 1205–1215.
- (11) Spencer, J. P.; Rice-Evans, C.; Williams, R. J. Modulation of pro-survival Akt/protein kinase B and ERK1/2 signaling cascades by quercetin and its in vivo metabolites underlie their action neuronal viability. *J. Biol. Chem.* **2003**, *278*, 34783–34793.
- (12) Motoshima, H.; Goldstein, B. J.; Igata, M.; Araki, E. AMPK and cell proliferation-AMPK as a therapeutic target for atherosclerosis and cancer. *J. Physiol.* **2006**, *574*, 63–71.
- (13) Koh, H.; Chung, J. AMPK links energy status to cell structure and mitosis. *Biochem. Biophys. Res. Commun.* **2007**, *362*, 789–792.
- (14) Moore, P. Connecting LKB1 and AMPK links metabolism with cancer. *J. Biol.* **2003**, *2*, 1–4.

- (15) Shaw, R. J.; Kosmatka, M.; Bardeesy, N.; Hurley, R. L.; Witters, L. A.; DePinho, R. A.; Cantley, L. C. The tumor suppressor LKB1 kinase directly activates AMP-activated kinase and regulates apoptosis in response to energy stress. *Proc. Natl. Acad. Sci. U.S.A.* **2004**, *101*, 3329–3335.
- (16) Hawley, S. A.; Boudeau, J.; Reid, J. L.; Mustard, K. J.; Udd, L.; Mäkelä, T. P.; Alessi, D. R.; Hardie, D. G. Complexes between the LKB1 tumor suppressor, STRAD α/β and MO25 α/β are upstream kinases in the AMP-activated protein kinase cascade. *J. Biol.* **2003**, *2*, 1–16.
- (17) Williamson, B.; Coniglio, J. G. The effects of pyridoxine deficiency and of caloric restriction on lipids in the developing rat brain. *J. Neurochem.* **1971**, *18*, 267–276.
- (18) Woods, A.; Vertommen, D.; Neumann, D.; Turk, R.; Bayliss, J.; Schlattner, U.; Wallimann, T.; Carling, D.; Rider, M. H. Identification of phosphorylation sites in AMP-activated protein kinase (AMPK) for upstream AMPK kinases and study of their roles by site-directed mutagenesis. *J. Biol. Chem.* **2003**, *278*, 28434–28442.
- (19) Hawley, S. A.; Davison, M.; Woods, A.; Davies, S. P.; Beri, R. K.; Carling, D.; Hardie, D. G. Characterization of the AMP-activated protein kinase from rat liver and identification of threonine 172 as the major site at which it phosphorylates AMP-activated protein kinase. *J. Biol. Chem.* **1996**, *271*, 27879–27887.
- (20) Hamilton, S. R.; O'Donnell, J. B., Jr.; Hammet, A.; Stapleton, D.; Habinowski, S. A.; Means, A. R.; Kemp, B. E.; Witters, L. A. AMP-activated protein kinase kinase: detection with recombinant AMPK α 1 subunit. *Biochem. Biophys. Res. Commun.* **2002**, *293*, 892–898.
- (21) Jin, Q.; Feng, L.; Behrens, C.; Bekele, B. N.; Wistuba, I. I.; Hong, W. K.; Lee, H. Y. Implication of AMP-activated protein kinase and Akt-regulated survivin in lung cancer chemopreventive activities of deguelin. *Cancer Res.* **2007**, *67*, 11630–11639.
- (22) Su, R. Y.; Chao, Y.; Chen, T. Y.; Huang, D. Y.; Lin, W. W. 5-Aminoimidazole-4-carboxamide riboside sensitizes TRAIL- and TNF α -induced cytotoxicity in colon cancer cells through AMP-activated protein kinase signaling. *Mol. Cancer Ther.* **2007**, *6*, 1562–1571.
- (23) Hwang, J. T.; Ha, J.; Park, I. J.; Lee, S. K.; Baik, H. W.; Kim, Y. M.; Park, O. J. Apoptotic effect of EGCG in HT-29 colon cancer cells via AMPK signal pathway. *Cancer Lett.* **2007**, *247*, 115–121.
- (24) Degtarev, A.; Boyce, M.; Yuan, J. A decade of caspases. *Oncogene* **2003**, *22*, 8543–8567.
- (25) Decker, P.; Muller, S. Modulating poly (ADP-ribose) polymerase activity: potential for the prevention and therapy of pathogenic situations involving DNA damage and oxidative stress. *Curr. Pharm. Biotechnol.* **2002**, *3*, 275–283.
- (26) Gown, A. M.; Willingham, M. C. Improved detection of apoptotic cells in archival paraffin sections: immunohistochemistry using antibodies to cleaved caspase 3. *J. Histochem. Cytochem.* **2002**, *50*, 449–454.
- (27) Duan, W. R.; Garner, D. S.; Williams, S. D.; Funckes-Shippy, C. L.; Spath, I. S.; Blomme, E. A. Comparison of immunohistochemistry for activated caspase-3 and cleaved cytokeratin 18 with the TUNEL method for quantification of apoptosis in histological sections of PC-3 subcutaneous xenografts. *J. Pathol.* **2003**, *199*, 221–228.
- (28) Resendes, A. R.; Majo, N.; Segales, J.; Espadamala, J.; Mateu, E.; Chianini, F.; Nofrarias, M.; Domingo, M. Apoptosis in normal lymphoid organs from healthy normal, conventional pigs at different ages detected by TUNEL and cleaved caspase-3 immunohistochemistry in paraffin-embedded tissues. *Vet. Immunol. Immunopathol.* **2004**, *99*, 203–213.
- (29) Jakob, S.; Corazza, N.; Diamantis, E.; Kappeler, A.; Brunner, T. Detection of apoptosis in vivo using antibodies against caspase-induced neo-epitopes. *Methods* **2008**, *44*, 255–261.
- (30) Shen, S.; Chen, Y.; Hsu, F.; Lee, W. Differential apoptosis-inducing effect of quercetin and its glycosides in human promyeloleukemic HL-60 cells by alternative activation of the caspase 3 cascade. *J. Cell Biochem.* **2003**, *89*, 1044–1055.
- (31) Lee, H. J.; Wang, C. J.; Kuo, H. C.; Chou, F. P.; Jean, L. F.; Tseng, T. H. Induction apoptosis of luteolin in human hepatoma HepG2 cells involving mitochondria translocation of Bax/Bak and activation of JNK. *Toxicol. Appl. Pharmacol.* **2005**, *203*, 124–131.
- (32) Singhal, R.; Yeh, Y. A.; Praja, N.; Olah, E.; Sledge, G. J.; Weber, G. Quercetin down-regulates signal transduction in human breast carcinoma cells. *Biochem. Biophys. Res. Commun.* **1995**, *208*, 425–431.
- (33) Nguyen, T.; Tran, E.; Nguyen, T.; Do, P.; Huynh, T.; Huynh, H. The role of activated MEK-ERK pathway in quercetin-induced growth inhibition and apoptosis in A549 lung cancer cells. *Carcinogenesis* **2004**, *25*, 647–659.
- (34) Yoshida, M.; Sakai, T.; Hosokawa, N.; Marui, N.; Matsumoto, K.; Fujioka, A.; Nishino, H.; Aoike, A. The effect of quercetin on cell cycle progression and growth of human gastric cancer cells. *FEBS Lett.* **1990**, *260*, 10–13.
- (35) Kaneuchi, M.; Sasaki, M.; Tanaka, Y.; Sakuragi, N.; Fujimoto, S.; Dahiya, R. Quercetin regulates growth of Ishikawa cells through the suppression of EGF and cyclin D1. *Int. J. Oncol.* **2003**, *22*, 159–164.
- (36) Ramos, S.; Alia, M.; Bravo, L.; Goya, L. Comparative effects of food-derived polyphenols on the viability and apoptosis of a human hepatoma cell line (HepG2). *J. Agric. Food Chem.* **2005**, *53*, 1271–1280.
- (37) Prives, C.; Hall, P. A. The p53 pathway. *J. Pathol.* **1999**, *187*, 112–126.
- (38) Sionov, R. V.; Haupt, Y. The cellular response to p53: the decision between life and death. *Oncogene* **1999**, *18*, 6145–6157.
- (39) Vousden, K. H.; Lu, X. Live or let die: the cell's response to p53. *Nat. Rev. Cancer* **2002**, *2*, 594–604.
- (40) Allen, R. T.; Hunter, W. J.; Agrawal, D. K. Morphological and biochemical characterization and analysis of apoptosis. *J. Pharmacol. Toxicol. Methods* **1997**, *37*, 215–228.
- (41) Benson, R. S.; Heer, S.; Dive, C.; Watson, A. J. Characterization of cell volume loss in CEM-C7A cells during dexamethasone-induced apoptosis. *Am. J. Physiol.* **1996**, *270*, 1190–1203.
- (42) Oda, K.; Arakawa, H.; Tanaka, T.; Matsuda, K.; Tanikawa, C.; Mori, T.; Nishimori, H.; Tamai, K.; Tokino, T.; Nakamura, Y.; Taya, Y. p53AIP1, a potential mediator of p53-dependent apoptosis, and its regulation by Ser46-phosphorylated p53. *Cell* **2000**, *102*, 849–862.
- (43) Matsuda, K.; Yoshida, K.; Taya, Y.; Nakamura, K.; Nakamura, Y.; Arakawa, H. p53AIP1 regulates the mitochondrial apoptotic pathway. *Cancer Res.* **2002**, *62*, 2883–2889.
- (44) Green, D. R.; Amarante-Mendes, G. P. The point-of-no-return: mitochondria, spasms and the commitment to cell death. *Results Probl. Cell Differ.* **1998**, *24*, 45–61.
- (45) Gunther, S.; Ruhe, C.; Derikito, M. G.; Bose, G.; Sauer, H.; Wartenberg, M. Polyphenols prevent cell shedding from mouse mammary cancer spheroids and inhibit cancer cell invasion in confrontation cultures derived from embryonic stem cells. *Cancer Lett.* **2006**, *250*, 25–35.
- (46) Gescher, A. J.; Steward, W. P. Relationship between mechanisms, bioavailability, and preclinical chemopreventive efficacy of resveratrol: a conundrum. *Cancer Epidemiol. Biomarkers Prev.* **2003**, *12*, 953–957.
- (47) Meng, X.; Maliakal, P.; Lu, H.; Lee, M. J.; Yang, C. S. Urinary and plasma levels of resveratrol and quercetin in humans, mice, and rats after ingestion of pure compounds and grape juice. *J. Agric. Food Chem.* **2004**, *52*, 935–942.
- (48) Manach, C.; Williamson, G.; Morand, C.; Scalbert, A.; Remesy, C. Bioavailability and bioefficacy of polyphenols in humans: I. Review of 97 bioavailability studies. *Am. J. Clin. Nutr.* **2005**, *81*, 230–242.
- (49) Asensi, M.; Medina, I.; Ortega, A.; Carretero, J.; Baño, M. C.; Obrador, E.; Estrela, J. M. Inhibition of cancer growth by resveratrol is related to its low bioavailability. *Free Radical Biol. Med.* **2002**, *33*, 387–398.
- (50) Ferrer, P.; Asensi, M.; Segarra, R.; Ortega, A.; Benlloch, M.; Obrador, E.; Varea, M. T.; Asensio, G.; Jordá, L.; Estrela, J. M. Association between pterostilbene and quercetin inhibits metastatic activity of B16 melanoma. *Neoplasia* **2005**, *7*, 37–47.
- (51) Fridman, J. S.; Lowe, S. W. Control of apoptosis by p53. *Oncogene* **2003**, *22*, 9030–9040.
- (52) Lee, Y. K.; Park, S. Y.; Kim, Y. M.; Lee, W. S.; Park, O. J. AMP kinase/cyclooxygenase-2 pathway regulates proliferation and apoptosis of cancer cells treated with quercetin. *Exp. Mol. Med.* **2009**, *41*, 201–207.